EEET ECOLOGICAL ENGINEERING & ENVIRONMENTAL TECHNOLOGY

Ecological Engineering & Environmental Technology, 2026, 27(3), 460–476
https://doi.org/10.12912/27197050/218415
ISSN 2719–7050, License CC-BY 4.0

Received: 2026.01.26
Accepted: 2026.02.25
Published: 2026.03.01

Immobilized peroxidase enzyme on quartz particles to bio oxidation of textile dye in a packed bed continuous system

Teba Saadi Hussein[1]

[1] Ministry of Education, Babylon Education Directorate, Iraq
E-mail: teba.saadi.ts@gmail.com

ABSTRACT

Discharge of synthetic dyes from industrial effluents represents a significant environmental concern due to their persistence, toxicity, and potential bioaccumulation in food chain. In present study, a sustainable bio catalytic system was developed using peroxidase extracted from discarded cabbage stems as an inexpensive and renewable enzyme source. Crude enzyme was covalently immobilized onto quartz particles to enhance operational stability and enable continuous application. Surface characterization of immobilized biocatalyst was performed using scanning electron microscopy (SEM), energy-dispersive X-ray spectroscopy (EDS), and Fourier-transform infrared spectroscopy (FTIR), confirming successful enzyme attachment. Immobilization yield reached 82%, and immobilized peroxidase exhibited optimal catalytic activity at pH 6.0 and 40 °C. Biocatalyst retained more than 37% of its initial activity after four consecutive degradation cycles. Influence of selected metal ions on enzymatic activity was also evaluated. Continuous degradation of reactive red dye was investigated in a packed-bed reactor operated for 38 h. Lower flow rates and higher catalyst loading significantly improved dye removal efficiency. Breakthrough behavior was successfully described using Bohart-Adams and Clark models ($R^2 > 0.99$), indicating good agreement between experimental and predicted data. These findings demonstrate that quartz-immobilized peroxidase derived from agricultural waste provides a viable and sustainable approach for continuous enzymatic treatment of dye-contaminated wastewater.

Keywords: cabbage stems peroxidase, covalent binding technique, peroxidase enzyme, quartz supports, reactive red 120.

INTRODUCTION

Water contamination has intensified over past century as a consequence of rapid industrialization and population growth [Kishor et al., 2021]. A major contributor to this problem is discharge of untreated industrial effluents containing synthetic dyes into aquatic ecosystems [Rahi et al., 2019]. These compounds are persistent, chemically stable, and often toxic, posing serious risks to aquatic organisms, environmental balance, and human health through potential entry into food chain [Chowdhary et al., 2020; Olisah et al., 2021].

Among synthetic dyes, azo dyes represent largest and most widely used class in textile industry due to their chemical stability and strong coloration properties [Ioannis et al., 2019]. However, their structural resistance to heat, light, and biodegradation makes them particularly difficult to remove using conventional treatment methods [Dineo et al., 2024]. Reactive red 120 (RR120), a widely applied water-soluble azo dye, has been reported to induce oxidative stress, cytotoxicity, and genotoxic effects in aquatic organisms. Such findings highlight urgent need for efficient and environmentally sustainable treatment strategies [Rania et al., 2022; Abdulrahman et al., 2021].

Conventional physicochemical treatment technologies are often costly, energy-intensive, and may generate secondary pollutants [Atiya et al., 2020]. In this context, enzyme-based biocatalytic systems have emerged as promising alternatives due to their high specificity, catalytic efficiency, and environmentally benign nature [Bilal et al., 2016]. Among oxidative enzymes, peroxidase (EC 1.11.1.7) has attracted considerable attention for

its ability to degrade a broad spectrum of phenolic and dye contaminants [Chiong et al., 2016].

Despite their catalytic potential, free enzymes suffer from limited operational stability, sensitivity to environmental conditions, and lack of reusability, which restricts their industrial application [Krainer and, Glieder 2015]. Enzyme immobilization is widely recognized as an effective strategy to overcome these limitations by enhancing stability, facilitating recovery, and enabling continuous processing [Maghraby et al., 2023]. Covalent immobilization, in particular, provides strong enzyme–support interactions, reduces enzyme leaching, and improves resistance to harsh physicochemical conditions [Jun et al., 2019].

Selection of an appropriate support material is crucial for maintaining catalytic activity while minimizing mass transfer limitations [Mohamad et al., 2015]. Inorganic supports offer mechanical strength, chemical stability, and suitability for continuous reactor configurations [Yang et al., 2022]. At same time, exploration of low-cost and renewable enzyme sources is essential for improving economic feasibility of biocatalytic wastewater treatment [Aziz et al., 2023].

Therefore, present study aims to develop a sustainable and cost-effective system for degradation of reactive red 120 using peroxidase extracted from discarded cabbage stems as a renewable enzyme source. Enzyme was immobilized onto quartz particles via covalent bonding to enhance operational stability and enable application in a packed-bed continuous reactor. Effects of pH, temperature, and reusability on catalytic performance were evaluated to assess feasibility of this approach for wastewater treatment applications.

MATERIALS AND METHODS

Substances and chemicals

Cabbage stems (*Brassica oleracea* var.) were collected from restaurant waste and used as a source of peroxidase. Potassium phosphate, sodium acetate, Tris-HCl, hydrogen peroxide (H_2O_2), pyrogallol, glutaraldehyde, and 3-aminopropyltriethoxysilane (APTES) were obtained from Sigma-Aldrich (USA) and used without further purification.

Reactive ted 120 (RR120), a triazine-based azo dye widely applied in textile industry, was supplied by a local textile facility (manufactured in Switzerland). Table 1 shows some characteristics and textile dye's chemical composition of textile dye employed in this investigation. A stock solution (1000 mg/L) was prepared by dissolving 1 g of dye in distilled water and diluting to 1 L. Working solutions were prepared by appropriate dilution [Sevtap, 2025]. Calibration standards (0–100 mg/L) were analyzed at 536 nm.

Table 1. Textile dye's chemical composition

Dye	Reactive Red 120
Molecular formula	$C_{44}H_{30}Cl_2N_{14}O_{20}S_6$
Molecular weight	1338.1 g/mol
Water solubility at 20 °C	60–70 (g/L)
Cas (chemical abstracts service)	61951-82-4
Chemical structure	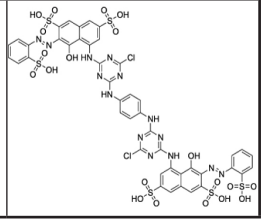

Quartz rock (QR) was used as an inorganic support for enzyme immobilization. Material was crushed, sieved to obtain particles of 0.85–1.0 mm (mesh 20), washed thoroughly with distilled water, and dried at 80 °C for 3 h prior to use shown in Figure 1.

Peroxidase extracted from cabbage stems was covalently immobilized onto quartz particles using silanization and glutaraldehyde crosslinking. Immobilized biocatalyst was subsequently applied for degradation of RR120 in batch and continuous systems.

Methods

Peroxidase was extracted from discarded cabbage stems (*Brassica oleracea* var.). Fresh stems (75 g) were washed, chopped, and homogenized in 375 mL of 0.2 M phosphate buffer (pH 6.0) for 25 min. Homogenate was filtered through two layers of sterile cheesecloth and centrifuged at 8000 rpm for 15 min. Resulting supernatant was further clarified by filtration through filter paper and collected as crude cabbage stem peroxidase (CSP). Extract was stored at 4–8 °C until further use.

Peroxidase activity was determined spectrophotometrically using pyrogallol as a substrate in presence of hydrogen peroxide. Enzymatic oxidation of pyrogallol produces purpurogallin, which was monitored at 420 nm (ε = 4400 M^{-1} cm^{-1}) at 25 °C.

Figure 1. Particles of quartz rock (0.85–1.0 mm)

Reaction mixture (3.6 mL total volume) consisted of 1.5 mL phosphate buffer (pH 6.0), 1.4 mL pyrogallol solution (50 mM), 0.4 mL H_2O_2 solution (25 mM), and 0.3 mL enzyme extract. Increase in absorbance at 420 nm was recorded at 1 min intervals using a UV–Vis spectrophotometer.

One unit (U) of peroxidase activity was defined as amount of enzyme catalyzing oxidation of 1 µmol of H_2O_2 per minute at 25 °C. Enzyme activity (U/mL) was calculated from linear change in absorbance using molar extinction coefficient of purpurogallin using Eq. (1). All measurements were performed in triplicate, and results are presented as mean values.

$$Activity\ \left(\frac{U}{mL}\right) = \frac{\left(\frac{dA}{dt}\right) \times AV \times DF}{EV \times \in_{420}} \quad (1)$$

[Pedrajas et al., 2020]

where: dA/dt: absorbency changes every minute (min^{-1}), AV: total volume (3.6 milliliters), DF: factor of dilution (1), EV: volume of enzyme (0.3 ml), $\in$ 420: At 420 nm, purpur ogallin absorptivity (4400 $ml \cdot \mu mol^{-1} cm^{-1}$).

Peroxidase was immobilized on qAuartz rock (QR) using a covalent binding technique. Quartz particles (1 g) were first functionalized with 0.5% (v/v) 3-aminopropyltriethoxysilane (APTES) by agitation on a mechanical shaker at ambient temperature for 4 h. Silanized support was then incubated with 2.5% (v/v) glutaraldehyde solution at room temperature for 8 h under gentle agitation to activate aldehyde groups for covalent bonding.

Crude cabbage stem peroxidase (CSP) was added at a concentration of 4 mg/mL, and mixture was incubated overnight at 4 °C under static conditions to allow enzyme attachment. Immobilized biocatalyst was subsequently washed and filtered to remove unbound enzyme. Filtrates were retained to determine residual peroxidase activity. Immobilization yield (IY%) Eq. (2) was calculated to quantify efficiency of enzyme binding to quartz support.

$$IY\ \% = \frac{Total\ activity\ of\ immobilized\ CLP}{Total\ activity\ of\ free\ CLP} * 100\% \quad (2)$$

[Hatakka, 1994]

Influence of pH on activity of immobilized peroxidase was evaluated using phosphate and acetate buffers in range of 4.0–9.0, adjusted in 0.5-unit increments. Immobilized biocatalysts were incubated in respective buffer solutions for 30 min at room temperature prior to activity measurement. Relative enzyme activity was determined to identify optimal pH for catalytic performance.

Temperature stability of immobilized enzyme was assessed by incubating biocatalyst at temperatures ranging from 25 to 80 °C for 30 min [Boudrant et al., 2020]. Enzyme activity was measured after incubation, and results were expressed as relative activity (RA) compared to maximum observed. Quartz-immobilized peroxidase retained high activity within 25–40 °C, while a gradual decline in activity was observed at higher temperatures.

RESULTS AND DISCUSSION

Peroxidase purification procedure from legs of cabbage plants was carried out using gel filtration chromatography, as shown in Table 2. When peroxidase is extracted from cabbage

Table 2. Purification parameters for CSP

Steps	Volume (ml)	Protein conc. (mg/ml)	Activity (U/ml)	Specific activity (U/mg)	Total activities (U)	Yield (%)	Purification fold
Crude	100	4.35	4977	1144	497700	100	1
Concentration by sucrose	28	4.81	7296	1516	204288	41	1.33
Sephadex G–150 gel filtration	46	1.73	4235	2448	194810	39	2.14

legs, a brown coloring occurs because legs contain a considerable amount of polyphenols. To produce a consistent enzyme product, purification procedure used Sephadex G150 gel filtration chromatography and ultrafiltration concentration. Significant peroxidase activity was shown in tubes 11–28, which were then used in further purification studies, as shown in Fig. 2. With a 2.14 purification factor in crude extract, application of this approach resulted in a notable increase in activity, which, as shown, produced a 39% yield. Results of gel filtration show a single band with a molecular weight of 55,000 Daltons; peroxidases in question have molecular weights between 30,000 and 60,000, which is similar to that of horseradish, artichoke leaves, and other dietary sources. Daltons [Cardinali et al., 2007].

Influence of pH on immobilized enzyme

pH alteration has an impact on biocatalyst action of enzymes due to modification of ionic properties within enzyme, which subsequently affects formation of active site. At an industrial level, estimation of impact pH on immobilized enzymes required careful consideration of their potential application [Timothy et al., 2023].

Peroxidase enzyme was homogenized using mortar with potassium phosphate buffer PH 6.5 at concentration 0.2 M and 1:5 (w: v) ratio at time of extract (30) min. to estimate activity, protein content and specific activity of enzyme at same procedure [Aziz et al., 2018]. Experiment implicated affecting pH of buffer solutions within range of 4.0 to 9.0, with an increase of half a pH unit.

Impact of pH on relative activity (RA) of immobilized (CSP) was exhibited in Figure 3 which observed that at pH 6, there is a significant increase in activity for all supports. However, in both acidic and basic regions, a decrease in activity is noticed. This is explained by ionic interaction between CSP and buffer's H^+ or OH^- ions, which in turn influences enzyme microenvironment [Ladole et al., 2020]. Decline in stability and activity at both high and low pH levels may be due to ionic variation in hem group. On other hand, redox potential falls with increasing pH, making substrate more susceptible to peroxidase oxidation. [Leon et al., 2002]. According to a prior study, peroxidase enzyme from green gram roots (Vigna radiata) showed best pH stability in the range of 5 to 7 [Basha and Prasada, 2017]. According [Matto et al., 2009], immobilized gourd peroxidase preparations had pH optima of pH 5,

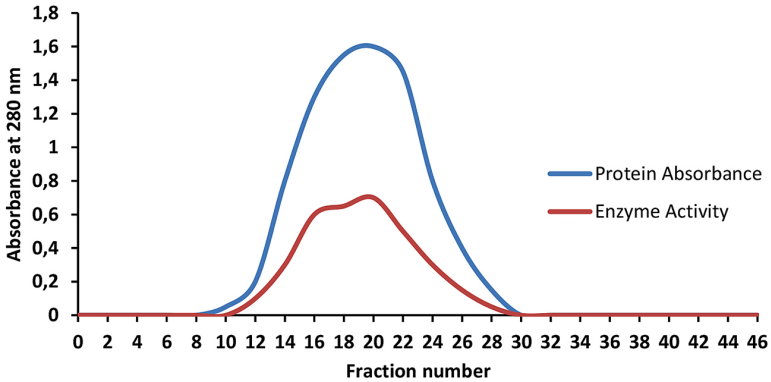

Figure 2. Elution profile for cabbage stems using gel filtration chromatography (20 ml/h flow rate, phosphate buffer 0.2 M at pH 6.5)

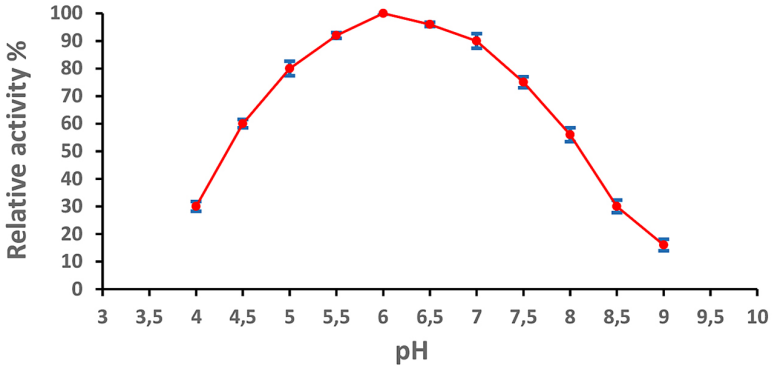

Figure 3. Impact of pH on immobilized biocatalysts by quartz rock

which was same as that of their soluble counterparts. When compared to other investigations, pH 5.5 produced highest peroxidase enzyme activity [Miranda et al., 2018].

Influence of temperature on immobilized enzyme

Impact of temperature on performance of immobilized (CSP) was assessed within a temperature domain from 25–80 °C, with each experiment lasting for a duration of 30 min. Findings were presented in relation to RA values immobilized (CSP), using mortar with potassium phosphate buffer PH 6.5 at concentration 0.2 M and 1:5 (w:v) ratio at time of extract 30 min. Peroxidase enzyme exhibits stability when immobilized using Quartz as support materials, across a temperature range of 25–40 °C, while maintaining its relative activity. Subsequently, enzyme exhibited decline in its enzymatic activity.

Results presented in Figure 4 indicate that optimum temperature was found to be 40 °C. Following that, high temperature causes enzyme molecules to become thermally denaturated, losing their active sites to catalyze substrate molecules. This causes enzyme's efficacy to rapidly decline until it reaches 80 °C. It is crucial to recognize that strong bond that forms between enzyme and activated support might cause conformational changes in biocatalyst. Immobilized peroxidase (CSP) with (QR) exhibited a retention of 45% of its enzymatic action when exposed to a temperature of 80 °C. This result is consistent with findings for immobilized (CSP) on different supports, red radish peroxidase enzyme extraction was demonstrated at 35°C in earlier research. [Diao et al., 2018]. On other hand, residual activity was measured through incubation at pH 6 at various temperature values extending from 20–80 °C to consider (CSP) thermal stability, which has noted a rise in temperature after immobilizing HRP with activated wool [Vishwasrao and Ananthanarayan, 2018]. Heat's effect on active site structure was blamed for denaturation and a decrease in enzyme activity.

Influence of metal salts

As illustrated in Figure 5, presence of metal salts at a concentration of 5 mM (in a 1:1 (v/v) ratio) impacts effectiveness of the peroxidase enzyme when it is incubated for 30 minutes and kept at 40 °C. Bioactivity of peroxidase was enhanced by presence of $FeSO_4$ and $ZnCl_2$ ions, resulting in 150% and 115% higher activities, respectively. However, enzyme activity was reduced by 20, 50%, and 53%, respectively, when $HgCl_2$, $AgNO_3$, and $CuCl_2$ ions were present. Residual activity of cabbage peroxidase did not significantly change for $MgSO_4$ and $AlCl_3$ ions, remaining at 90% and 91%, respectively. Different metallic ions affect enzymes differently, which provides information about inhibition or activation, in line with previously published research [Asadullah et al., 2022]. Iron and zinc are examples of heavy metal ions that increase peroxidase effectiveness, possibly by strengthening presence of iron (III) atoms (Fe^{3+}) near active site of enzyme [Munir et al., 2023] and these findings concur with earlier studies that show Fe^{3+} activates pure peroxidase activity [Al-Senaidy and Ismael, 2011]. Mercury and silver quickly react with thiol (SH) and amine (NH) groups in enzyme's active site, causing irreversible inactivation, as well as with carboxyl groups (COO) at or close to active site, preventing contact, in imidazole ring of histidine. Results of this investigation are consistent with those of [Altın et al., 2017].

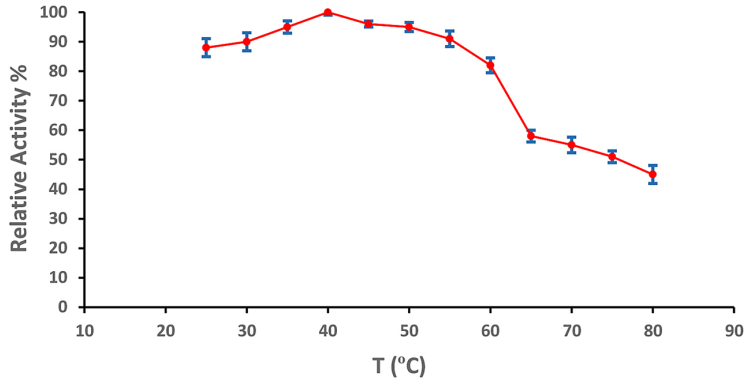

Figure 4. Impact of temperature on immobilized biocatalysts by quartz rock

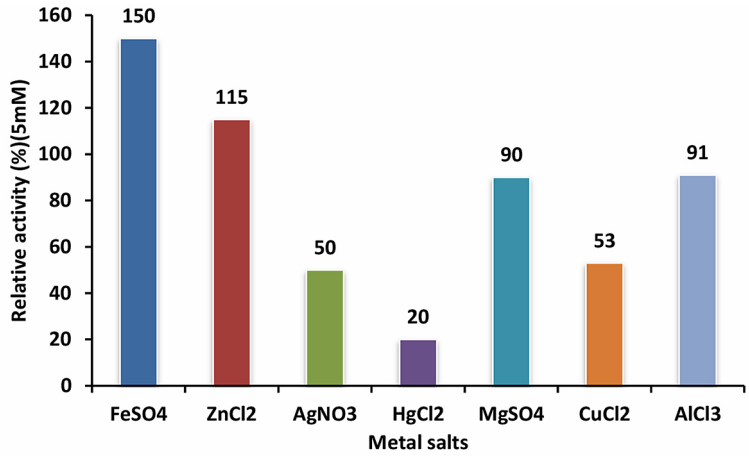

Figure 5. Effects of metal ions on enzyme activity

Reusability of enzyme

Reutilization of immobilized enzymes is necessary due to significant expense associated with soluble enzymes. Decrease in activity that is observed upon repeated use can potentially be ascribed to inhibition of enzyme activity resulting from leaching of enzymes during repetitive washing procedure, as well as damage inflicted upon supports [Maryam et al., 2022].

Immobilized (CSP) preparation was subjected to extraction and rinsing using a 0.2 M phosphate buffer solution with a pH of 6. Initial activity measurement was designated as control (100%) for subsequent calculation of remaining percentage activity after each subsequent use [Ali and Husain, 2018]. Reusability cycles are depicted in Figure 6, cabbage stems peroxidase, which was immobilized in (QR) by (CBT), exhibited maintenance of 85% in terms of initial activity, during a double cycle. However, in fourth cycle, remaining action decreased to 37%,

In a previous study, for immobilized soybean peroxidase reuse was done for four cycles, where removal efficiency was reduced to half original efficiency [Chagas et al., 2015]. In another previous study, reutilization experiments demonstrated that more than 40% of original activity of immobilized HRP could be retained after seven recycling cycles [Bilal et al., 2016].

Scanning electron microscopy

Scanning electron microscopy (SEM) was used to examine solid support (quartz rocks) samples. Surface morphology of original, altered, and immobilized particles was examined using SEM (Fessem Tescan Mira 3, French). Solid support samples were subjected to examination, and resulting images were analyzed. With an accelerating voltage of 15 kilovolts, microscope was used. Onto samples, a coating with a thickness of 2 µm was sprayed. First immobilized support was dried and vacuum-coated

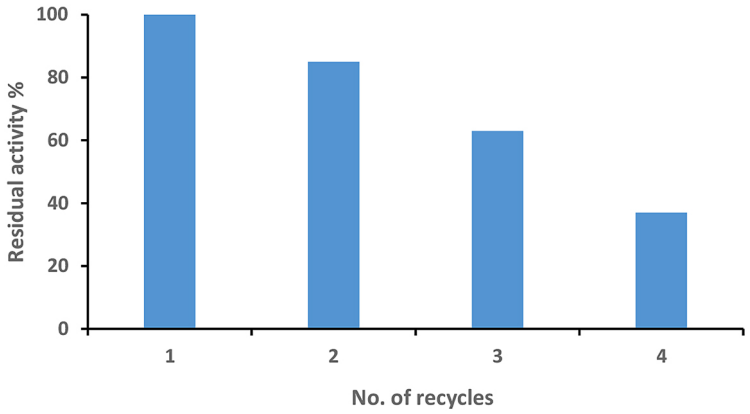

Figure 6. Reusability cycles of immobilized (CSP) enzyme

with nanogold to improve electrical conductivity before scanning. SEM images revealed morphological changes and increased surface roughness after immobilization, suggesting successful enzyme attachment to quartz surface. Immobilization yield (IY = 82 ± 0.41%) confirmed this result, as shown in Figure 7.

Energy dispersive spectrometer

Energy dispersive spectrometer (EDS) instrument is extensively employed for microscopic analysis in various fields. Microchemical analysis for (QR) support was conducted by utilization of energy-dispersive χ-ray spectroscopy EDS in combination with scanning electron microscopy SEM is employed. EDS was employed to analyze alterations in support characteristics before and after immobilization. Figure 8 (A, B) illustrates various EDS techniques. Findings indicated that there was an approximate 16 wt% decrease in weight of element Si, followed by a 8 wt% increase in weight of element O, and element C decreased about 8 wt% in region of initial support when compared to quartz after immobilization, which confirmed successful immobilization as listed in Table 3.

Furthermore, EDS showed that elements Na, Mg, K, and Fe were absent from original supports, but they were discovered following enzyme's immobilization, confirming presence of peroxidase on supports and indicating a successful immobilization process [Wang et al., 2015].

Fourier transform infrared analysis

Function group analysis was performed with Fourier transform infrared analysis (FTIR) spectroscopic over range from 500–4000 cm^{-1}, using

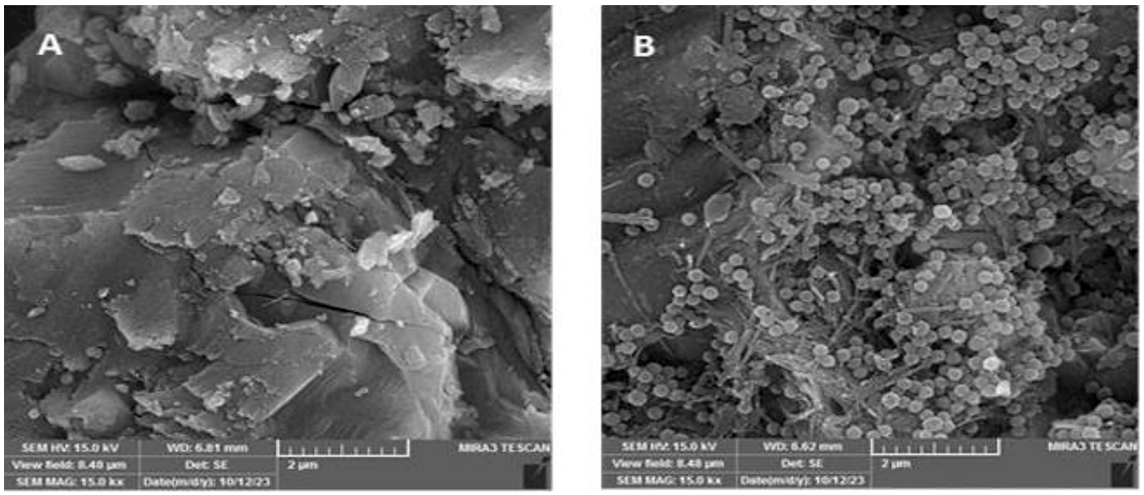

Figure 7. SEM images supports/immobilized biocatalysts before and after immobilized (A, B) QR support respectively

Table 3. EDS weight percent for three types of support before and after immobilized

QR support	Before immobilization				
	C (W%)	O (W%)	Si (W%)	S (W%)	Ca (W%)
	12.96	27.71	48.81	10.97	-
	After immobilization				
	C (W%)	O (W%)	Si (W%)	S (W%)	Ca (W%)
	4.49	35.32	32.11	12.22	10.10

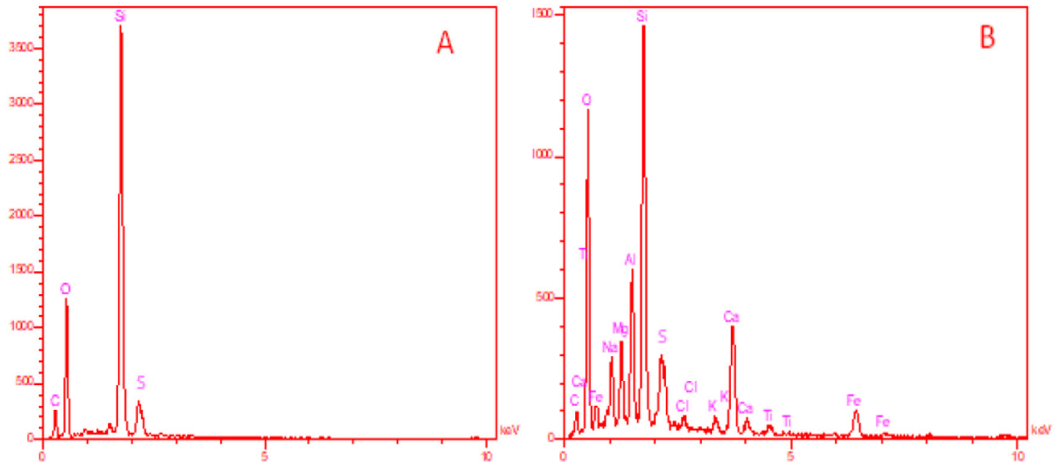

Figure 8. EDS spectrum photographs of supports (A, B) QR before and after immobilized enzyme

an instrument supplied by Perkin Elmer spectrophotometer, England.

FTIR analysis shows in Figure 9 illustrate peroxidase enzyme before and after decolorization of RR120 pollutant. It can be seen that some functional group peaks are responsible for sorption. FTIR spectra of immobilization of crude peroxidase enzyme was in a range of 500–4000 cm^{-1} to find functional groups are potential for sorption procedures, that shows a number of sorption peaks, indicating composition nature of matter analyzed. FTIR spectrum depending on bio sorbent were assigned to different groups, and various bonds, according to private waves numbers at cm^{-1}.

Broad intense absorption peaks at differences in waves 3632, and 3430 cm^{-1} are indicative of presence of (O-H) hydroxyl strength vibration. Peaks differences in waves are because of (O-H) vibration, while peak of 2857 cm^{-1} is indicative of presence of alkyne groups (C-H). (C-O) group vibration can be used to identify peak values of 1340, and 1150 cm^{-1}.

Peaks at 1770 cm^{-1}, are indicative of presence of strong intensity of (C=O) carbonyl group. Functional carbonyl and hydroxyl groups can determine degradation processes [Chen et al., 2021]. Absorption peaks at 554 cm^{-1} represent Si-OH group, while a band at 720, 860 cm^{-1} represents Si-O-Si group as illustrated in Figure 6. Decrease in different functional groups on support after immobilization and after completing degradation of pollutants indicates that enzyme entered process of breaking down pollutants and exited maintaining its structure [Brányik et al., 2004].

Column experiments for removal dye were done to test activity of peroxidase enzyme at certain conditions (pollutant concentration, flow rate, packed height) depending on efficiency of pollutant removal as an indicator. Column were made from Perspex cylinders 0.4 m long and 3 cm in diameter, and samples were collected from port at 5, 10, and 15 cm, and supplied with plastic valves. Immobilized peroxidase particle were packed into column, with use of optimal parameters obtained for decolorization, pollutant solution was gradually pumped out, fed from bottom of column filled with peroxidase enzyme individually using peristaltic pump with steady state flow rate 0.5, 1, and 1.5 ml/min. flow of pollutant solution will push air upwards and will prohibit presence of air between immobilized peroxides particles, samples were taken from a glass bottle filled with pollutant

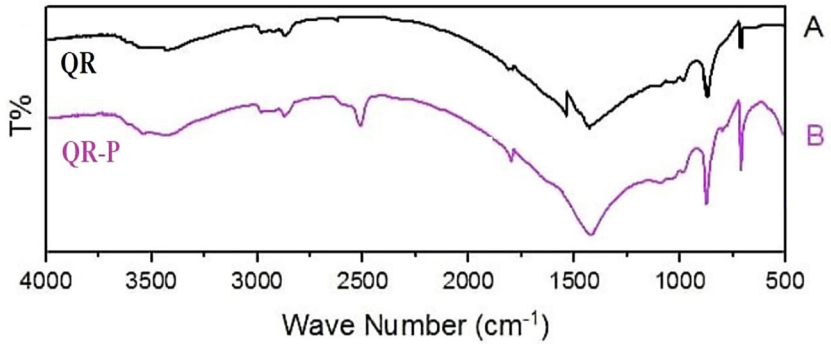

Figure 9. FTIR spectra results of: (A) raw QR, (B) QR with enzyme

water. Experiment persisted until concentration of treated solution equaled feedconcentration. A schematic represented experimental equipment is shown in Figures 10, and 11. All experimental conditions are summarized in Table 4.

Effect of bed height

At a concentration of 10 mg/l, flow rate 0.5 ml/min effect of bed height at port 1 (5 cm), port 2 (10 cm), and port 3 (15 cm) were examined to find percentage of degradation of pollutants. Figure 12 RR120 prove that there might be a noticeable delay in development of curve due to increased amount of biosorbent material packed in column. This means that higher depth can prepare a suitable duration for molecules diffuse within voids of biosorbent grains and this can increase biodegradation of pollutant. These figures show typical S-shape graphs "known as breakthrough curves" where both breakthrough time and collected effluent increased with increasing bed depth. By changing bed depth from 5 cm (port 1) to 15 cm (port 3), "breakthrough time" can noticeably increase. For example, RR120 pollutant time of degradation increased from 2 to 6 h at a percentage of 98% with increase in bed depth from 5 cm to 15 cm as shown in Figure 12.

It is important to note that increasing bed depth will decrease bed's capacity to degrade for a given intake concentration since pollutant may be dispersed over a larger surface area at a deeper depth [Qili et al., 2021]. Time required to attain exhaustion of biosorbent is known as exhaust time. Because there are more active sites for oxidation at higher bed heights, this time increases. Current findings were consistent with those documented in earlier research [Teba and Ayad, 2023; Arunachalam et al., 2021; Natália et al., 2020].

Table 4. Packed bed experimental conditions

Parameter	Value
Flow rate (ml/min)	0.5,1,1.5
Packed height (cm)	5, 10, 15
Concentration (mg/l)	10, 25, 50
Temperature (°C)	40
pH	6

Effect of inlet concentration

Influence of different concentrations of adopted pollutant (10, 25, 50) mg/l through bed height of 15 cm and discharge 0.5 mL/min was investigated for ports 1, 2, and 3. Results indicated that low concentrations achieve higher decolorization efficiency due to decrease in pollutant molecules and due to complete saturation of enzyme with dye at higher concentrations as presented in Fig. 13. Many researchers also reported decreased in degradation at higher pollutant concentrations [Christelle et al., 2023; Khaled et al.,2022].

Effect of flowrate

Effect of water flow rate on oxidation of pollutants onto immobilized enzymes was monitored by applying three rate values; 0.5, 1 and 1.5 ml/min. As plotted in Figure 14, was based on C_o 10 mg/l and a bed height 15 cm. Results show that RR120 achieve complete decolonization till 6 h then reduce to 98%.

Decolonization percentage decreased as flow rate increased to 1 and 1.5 ml/min. This suggests that in a packed-bed reactor, decreasing flow velocity lengthens time that enzyme and dye are in contact. Increase in discharge can be accompanied by reduction in breakthrough time. Thus, increasing flow velocity can reduce adhesion time

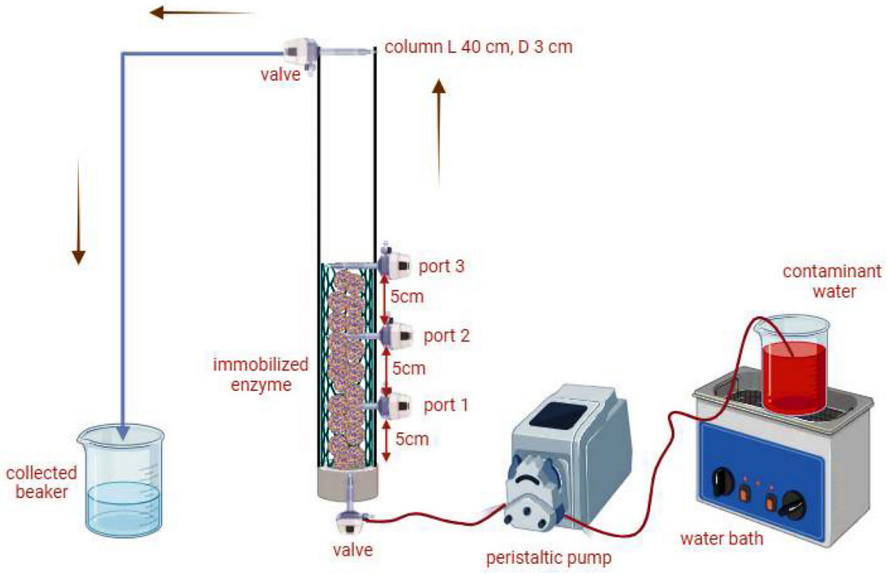

Figure 10. Schematic diagram of packed bed reactor

Figure 11. Laboratory system of packed-bed reactor

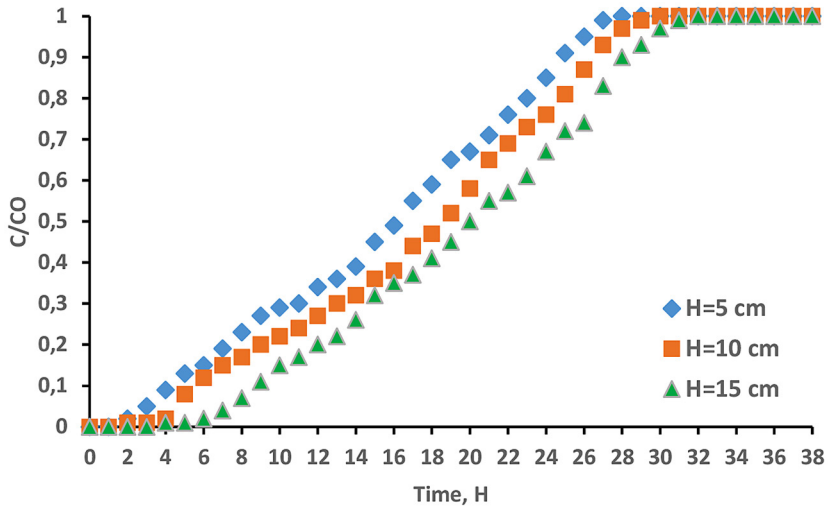

Figure 12. Measured breakthrough curves for different bed high at flowrate of 0.5 mL/min, C 10 mg/l

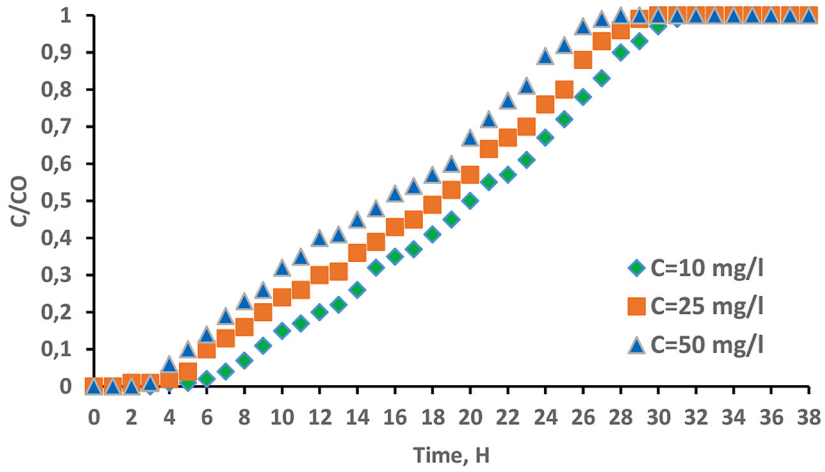

Figure 13. Measured breakthrough curves for different inlet concentrations of RR120 at flowrate of 0.5 mL/min, H 15 cm

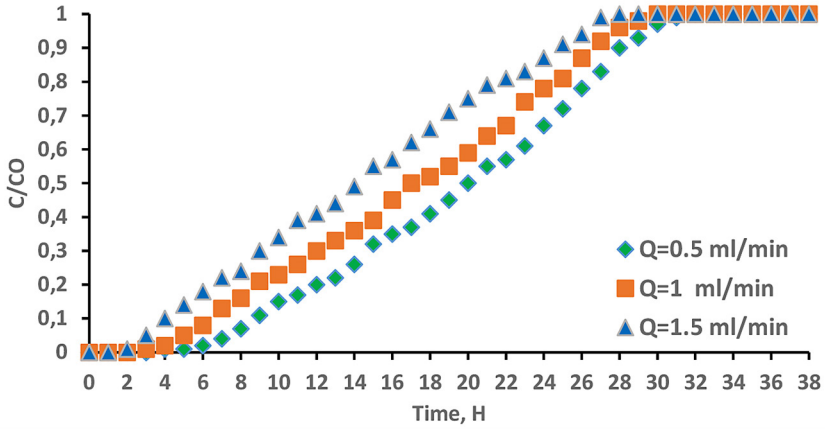

Figure 14. Measured breakthrough curves for different flowrate of RR120 at flowrate at H 15, C 10 mg/l

between solute and catalyst particles and this leads to an obvious reduction in removal percentage [Aaron and Runping, 2022]. Present results were in agreement with those reported in previous studies [Suppanat et al., 2025; Sikha et al., 2025; Omdehghiasi et al., 2024].

Modelling of breakthrough curves

In this study, Bohart-Adams and Clark models were employed to analyze breakthrough behavior of textile dye bio-oxidation in a continuous packed-bed reactor containing peroxidase enzyme immobilized on quartz particles. These models were selected because they are well established for describing mass transfer and reaction kinetics in fixed-bed systems and enable quantitative evaluation of column performance. Bohart-Adams model was used to describe initial breakthrough region, where dye removal is primarily governed by availability of active enzyme sites and external mass transfer, allowing estimation of kinetic rate constant and maximum bed capacity [Qili et al., 2024]. In contrast, Clark model, which incorporates saturation-type kinetics, was applied to represent entire breakthrough curve and more accurately capture enzyme-controlled oxidation and gradual loss of catalytic activity over time [Aguirre et al., 2023]. Fitting these models to experimental data provides insight into governing mechanisms of dye bio-oxidation, validates experimental results, and offers essential parameters for predicting reactor performance and scaling up continuous treatment system [Khim et al., 2023].

Breakthrough curves measured along immobilized peroxidase enzyme on quartz particles in packed bed at different discharges and inlet

a) Q=0.5 mL/min, Co= 10 mg/L, H=15 cm

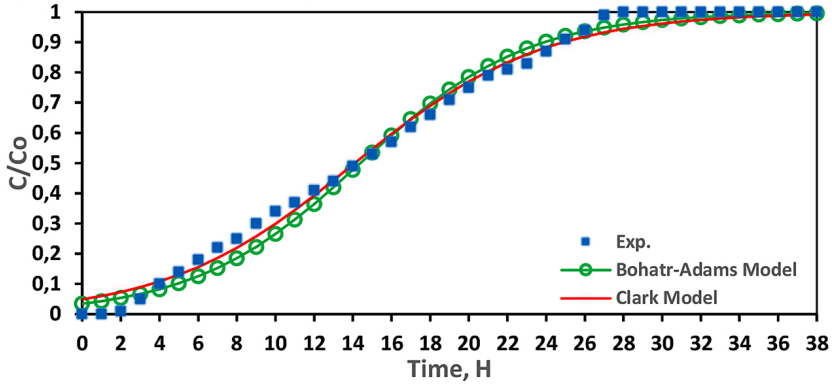

b) Q=0.5 mL/min, Co= 25 mg/L, H=15 cm

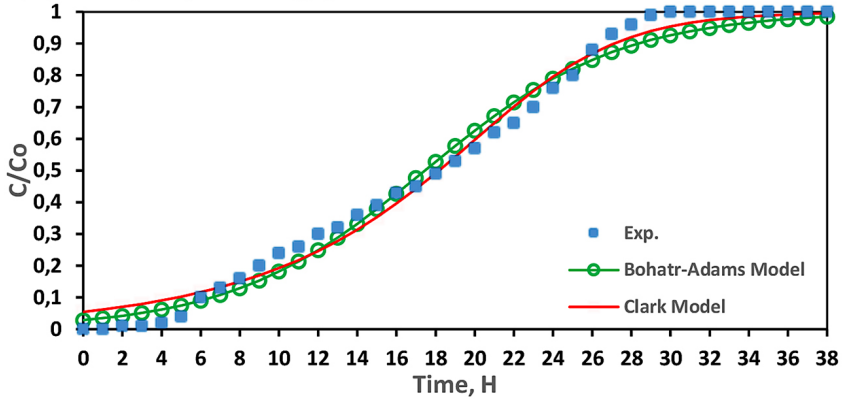

c) Q=0.5 mL/min, Co= 50 mg/L, H=15 cm

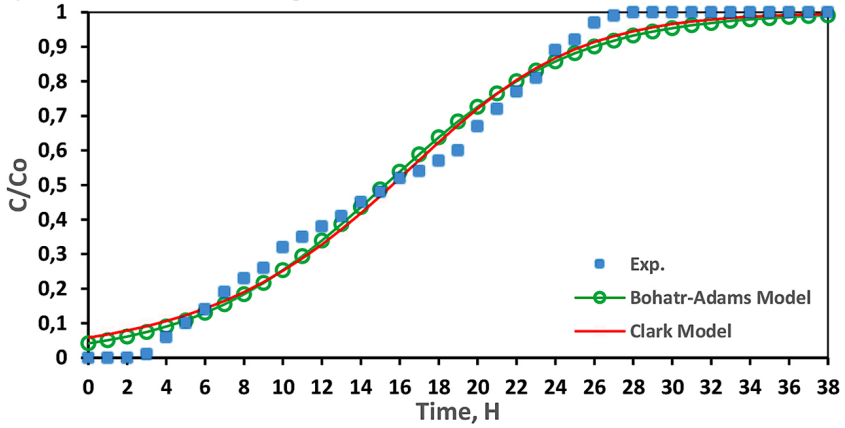

d) Q=1 mL/min, Co= 10 mg/L, H=15 cm

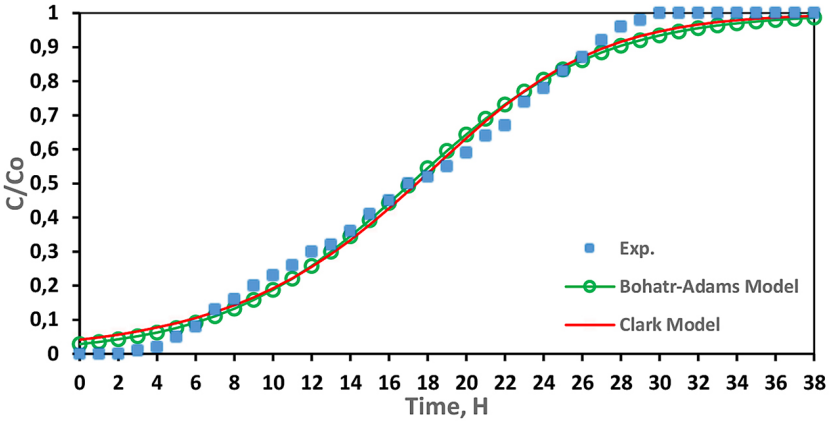

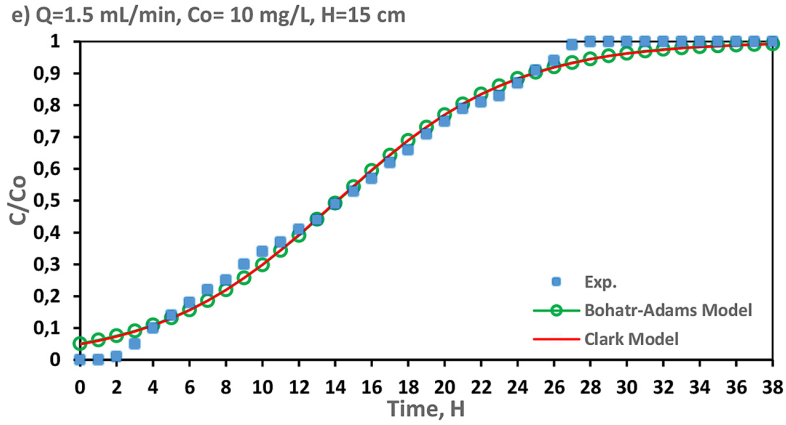

Figure 15. Breakthrough models for fitting measurements of effluent C/C_{in} for various values of flowrate and inlet RR120 concentrations at H = 15 cm

concentrations for depths ranging from 5 to 15 cm are formulated by number of familiar models as plotted in Figures 10. Models are represented by Bohart-Adams and Clark models expressions which simulated trends of curves at ports 1, 2, and 3. Solver option in Microsoft Excel 2016 for nonlinear regression was applied to determine fit between these models and experimental

Table 5. Results for using adopted models to fit measured RR120 breakthrough curves at H = 15 cm for various inlet concentrations and a flowrate of 0.5 mL/min

Model	Parameter	H=15 cm		
		10	25	50
Bohart-Adams	KC_o	0.232	0.202	0.379
	KN_oZ/U	3.333	3.526	0.206
	R^2	0.989	0.990	0.987
	SSE	0.054	0.988	0.987
Clark	A	2.668	10.013	5.857
	r	0.202	0.301	0.249
	n	1.934	3.365	2.633
	R^2	0.993	0.990	0.987
	SSE	0.037	0.059	0.073

Table 6. Results of fitting measured RR120 breakthrough curves using models that were used at H = 15 cm for various flow rates and an inlet concentration of 10 mg/L

Model	Parameter	H=15 cm		
		0.5	1	1.5
Bohart-Adams	KC_o	0.232	0.206	0.206
	KN_oZ/U	3.333	3.525	3.525
	R^2	0.989	0.992	0.978
	SSE	0.054	0.052	0.336
Clark	A	2.668	5.209	5.810
	r	0.202	0.244	0.243
	n	1.934	2.542	2.542
	R^2	0.993	0.992	0.972
	SSE	0.037	0.049	0.342

measurements. Outputs of fitting process included parameters of models and statistical measures for goodness of matching between measured and predicted values of C/C_{in} have been listed in Tables 5 and 6. It is clear than Bohart-Adams, and Clark models accurately describe experimental measurements with $R^2 > 0.993$ and SSE < 0.998.

Bohart-Adams model

Adams-Bohart model is a classical breakthrough curve model used to describe adsorption of a solute from a fluid (often water or air) onto a solid adsorbent in a fixed-bed column, and is mainly applied to initial part of breakthrough curve, where external mass transfer resistance is dominant [Bringas et al., 2023]:

$$\frac{C}{C_o} = \frac{1}{1 + \exp\left(KN_o\frac{Z}{U} - KC_o t\right)} \tag{3}$$

where: N_0 is solute content at saturation level (mg/L), Z is bed depth (cm), t is elapsed time (min), U is flow rate (cm/min), and K is kinetic constant (L/g/min).

Clark model

Teba and Ayad (2024) established a breakthrough curve simulation suitable for column. Freundlich isotherm and mass-transfer concept were utilized in this created model to portray relationship for breakthrough curve as follow [Madan et al., 2019]:

$$\left(\frac{C}{C_o}\right)^{n-1} = \frac{1}{1 + A \cdot e^{-rt}} \tag{4}$$

where: n is Freundlich model's exponent as well as, r and A are constants from kinetic formula.

CONCLUSIONS

A practical and sustainable approach was achieved through utilization of low-cost resources and implementation of efficient methods, resulting in an environmentally safe and economically viable process for enzyme recovery. Peroxidase bioenzyme has been extracted, purified, and biochemically examined from cabbage stems waste in this study. peroxidase enzyme immobilized on QR support. This method was used as best method of immobilization because it preserves stability of enzyme and its internal structure and prevents it from leaking. CSP has thermostability, high relative activity, and stability throughout an extensive pH range. pH 6.0 was illustrated to be optimal range for all immobilized biocatalysts. Concerning biocatalyst optimum temperature, outcome of increased temperature for biocatalyst with all support remains at same value 40 °C as optimum temperature of bioenzyme, when temperature reached 80 °C, QR support maintained approximately 45% of original enzyme efficiency, which is highest remaining percentage of enzyme efficiency. Regarding of reuse, immobilized enzyme on QR exhibited a maintenance of 85%, in terms of initial activity during double cycle. SEM was utilized to analyze surface morphology of initial, and immobilized particles.

Notably, distinct alterations on particle surface were observed. EDS was employed to analyze alterations of elements on supports before and after immobilization. Optimal flow rate, bed height, and dye inflow concentration were determined by tests in immobilized catalyzed packed bed reactors to find best conditions for pollutant degradation. Results showed that these parameters were 0.5 ml/min, 15 cm and 10 mg/L respectively. Removal efficiency in continuous mode increased with increase bed height, while decrease with increasing flow rate and pollutant concentration. Findings demonstrated potential of utilizing crude enzyme directly, eliminating necessity for costly and time-consuming purification processes. Study is an introduction to developing enzyme-immobilized technology, its widespread use in treating chemical industrial pollutants, and many chemical processes in which enzymes play an important role.

Long breakthrough period under continuous flow suggests that enzyme-immobilized adsorbent maintains high dye uptake efficiency with slow saturation at lower influent concentrations – which may outperform conventional adsorbents in low-strength effluent polishing applications.

Acknowledgments

Authors are thankful to Iraqi textile factory and University of Babylon, College of Engineering, Environmental Engineering Department for Their cooperation. Our sincere gratitude to Research and Development Laboratories at College.

REFERENCES

1. Aaron AA, Runping H. (2022). A novel biocomposite based on peanut husk with antibacterial properties for the efficient sequestration of trimethoprim in solution: Batch and column adsorption studies. *Colloids and Surfaces A: Physicochemical and Engineering Aspects*. 635, 128051. https://doi.org/10.1016/j.colsurfa.2021.128051
2. Abdulrahman, A.N., Ahmed, A., & Gordon, M. (2021). Removal of phenols and dyes from aqueous solutions using graphene and graphene composite adsorption: A review. *Journal of Environmental Chemical Engineering*, 9(5), 105858. https://doi.org/10.1016/j.jece.2021.105858
3. Aguirre, C. S., Leyva, R. R., Ocampo, P. R., Aguilar, M. C.G., Flores, C.J.V., & Medellín, C. N.A. (2023). Mathematical modeling of breakthrough curves for 8-hydroxyquinoline removal from fundamental equilibrium and adsorption rate studies. *Journal of Water Process Engineering*, 54, 103967. https://doi.org/10.1016/j.jwpe.2023.103967
4. Ali, M., & Husain, Q. (2018). Guar gum blended alginate/agarose hydrogel as a promising support for the entrapment of peroxidase: Stability and reusability studies for the treatment of textile effluent. *International Journal of Biological Macromolecules*, 116, 463-471. DOI: 10.1016/j.ijbiomac.2018.05.037
5. Al-Senaidy, A.M., & Ismael, M.A. (2011). Purification and characterization of membrane-bound peroxidase from date palm leaves (*Phoenix dactylifera* L.). *Saudi Journal of Biological Sciences*, 18 (3), 293-298. https://doi.org/10.1016/j.sjbs.2011.04.005
6. Altın, S., Tohma, H., Gülçin, İ., & Köksal, E. (2017). Purification, characterization, and inhibition sensitivity of peroxidase from wheat (*Triticum aestivum* ssp. vulgare). *International Journal of Food Properties*, 20 (9), 1949-1959. https://doi.org/10.1080/10942912.2016.1225308
7. Arunachalam, T., Rajarathinam, N., & Raja, S. (2021). Continuous fixed-bed biosorption process: A review. *Chemical Engineering Journal Advances*, 8, 100188. https://doi.org/10.1016/j.ceja.2021.100188
8. Asadullah, L.K., Kuaanan, T., Zahid, N.Q., Chowdhury, M.S., & Murat, Y. (2022). Elimination of selected heavy metals from aqueous solutions using biochar and bentonite composite monolith in a fixed-bed operation. *Journal of Environmental Chemical Engineering*, 10(1), 106993. https://doi.org/10.1016/j.jece.2021.106993
9. Atiya, M.A., Ridha, M. J., & Saheb, M.A. (2020). Removal of Aniline Blue from Textile Wastewater using Electrocoagulation. *Iraqi Journal of Science*, 2797-2811. https://doi.org/10.24996/ijs.2020.61.11.4
10. Aziz, G.M., Al-Sa'ady, A.J., & Bedan, D. S. (2018). Characterization and immobilization of purified polyphenol oxidase extracted from banana peel. *Iraqi Journal of Biotechnology*, 17(2). https://jige.uobaghdad.edu.iq/index.php/IJB/article/view/42
11. Aziz, G.M., Hussein, S.I., Ridha, M.J., Mohammed, S.J., Abed, K.M., Muhamad, M.H., & Hasan, H.A. (2023). Activity of laccase enzyme extracted from Malva parviflora and its potential for degradation of reactive dyes in aqueous solution. International Society of Biocatalysis and Agricultural Biotechnology (ISBAB), https://doi.org/10.1016/j.bcab.2023.102671.
12. Basha, S.A., & Prasada, R.U.J. (2017). Purification and characterization of peroxidase from sprouted green gram (*Vigna radiata*) roots and removal of phenol and p-chlorophenol by immobilized peroxidase. *Journal of the Science of Food and Agriculture*, 97(10), 3249-3260. DOI: 10.1002/jsfa.8173
13. Bilal, M., Iqbal, H.M.N., Shah, S.Z.H., Hu, H., Wang, W., & Zhang, X. (2016). Horseradish peroxidase-assisted approach to decolorize and detoxify dye pollutants in a packed bed bioreactor. *J. Environ. Manag*. http://dx.doi.org/10.1016/j.jenvman.2016.09.040.
14. Bilal, M., Iqbal, M., Hu, H., & Zhang, X. (2016). Mutagenicity and cytotoxicity assessment of biodegraded textile effluent by Ca-alginate encapsulated manganese peroxidase. *Biochemical Engineering Journal*, 109, 153-161. https://doi.org/10.1016/j.bej.2016.01.020
15. Boudrant, J., Woodley, J.M., & Fernandez, L.R. (2020). Parameters necessary to define an immobilized enzyme preparation. *Process Biochemistry*, 90, 66-80. https://doi.org/10.1016/j.procbio.2019.11.026
16. Brányik, T., Vicente, A., Oliveira, R., & Teixeira, J. (2004). Physicochemical surface properties of brewing yeast influencing their immobilization onto spent grains in a continuous reactor. *Biotechnology and bioengineering*, 88 (1), 84-93. https://doi.org/10.1002/bit.20217
17. Bringas, A., Bringas, E., Ibañez, R., San, R. M.F. (2023). Fixed-bed columns mathematical modeling for selective nickel and copper recovery from industrial spent acids by chelating resins. *Separation and Purification Technology*, 313, 123457. https://doi.org/10.1016/j.seppur.2023.123457
18. Cardinali, A., Sergio, L., Di, V.D., Linsalata, V., Fortunato, D., Conti, A., & Lattanzio, V. (2007). Purification and characterization. *Journal of the Science of Food and Agriculture*, 87(7), 1417-1423. DOI:10.1002/jsfa.2882
19. Chagas, P.M.B., Torres, J.A., Silva, M.C., & Corrêa, A.D. (2015). Immobilized soybean hull peroxidase for the oxidation of phenolic compounds in coffee processing wastewater. *International Journal of Biological Macromolecules*, 81, 568-575. https://doi.org/10.1016/j.ijbiomac.2015.08.061
20. Chen, G., An, X., Li, H., Lai, F., Yuan, E., Xia, X., & Zhang, Q. (2021). Detoxification of azo dye Direct Black G by thermophilic *Anoxybacillus* sp. PDR2 and its application potential in bioremediation.

Ecotoxicology and Environmental Safety, 214, 112084. https://doi.org/10.1016/j.ecoenv.2021.112084

21. Chiong, T., Lau, S.Y., Lek, Z.H., Koh, B.Y., & Danquah, M.K. (2016). Enzymatic treatment of methyl orange dye in synthetic wastewater by plant-based peroxidase enzymes. *Journal of Environmental Chemical Engineering*, 4, 2500–2509. https://doi.org/10.1016/j.jece.2016.04.030.
22. Chowdhary, P., Bharagava, R.N., Mishra, S., & Khan, N. (2020). Role of industries in water scarcity and its adverse effects on environment and human health. Environmental Concerns and Sustainable Development. Volume 1: Air, Water and Energy Resources. 235-256. https://link.springer.com/chapter/10.1007/978-981-13-5889-0_12
23. Christelle, R., Andrea, P., Yves, A., Audrey, V., & Sary, A. (2023). Adsorption of ibuprofen from aqueous solution onto a raw and steam-activated biochar derived from recycled textiles insulation panels at end-of-life: Kinetic, isotherm and fixed-bed experiments. *Journal of Water Process Engineering*, 53, 103830. https://doi.org/10.1016/j.jwpe.2023.103830
24. Diao, M., Dibala, C.I., Ayékoué, B.N., & Dicko, M.H. (Biochemical). (2018). characterization of Burkina red radish (Raphanus sativus) peroxidase. *Journal of Applied Biosciences*, 125, 12518-12530. https://doi.org/10.4314/jab.v125i1.2
25. Dineo, A.B., Bulelwa, N., & Fumani, D.M. (2024). Photocatalysis as a pre-discharge treatment to improve the effect of textile dyes on human health: A critical review. *Heliyon*, 10(20), e39316. https://doi.org/10.1016/j.heliyon.2024.e39316
26. Hatakka, A. (1994). Lignin-modifying enzymes from selected white-rot fungi: production and role from in lignin degradation. *FEMS Microbiology Reviews*, 13(2-3), 125-135. https://www.sciencedirect.com/science/article/abs/pii/0168644594900760
27. Ioannis, A., Ioannis, P., Ahmad, H.B., Dimitrios, A.G., Artis, R., Muhammad, U., Leticia, B.E., Yaoyu, Z., Juan, C.C., Avelino, N.D., & Éder, C.L. (2019). Agricultural biomass/waste as adsorbents for toxic metal decontamination of aqueous solutions. *Journal of Molecular Liquids*, 295, 111684. https://doi.org/10.1016/j.molliq.2019.111684
28. Jun, L.Y., Yon, L.S., Mubarak, N., Bing, C.H., Pan, S., Danquah, M.K., & Khalid, M. (2019). An overview of immobilized enzyme technologies for dye and phenolic removal from wastewater. *Journal of Environmental Chemical Engineering*, 7, 102961. https://doi.org/10.1016/j.jece.2019.102961
29. Khaled, A.Z., María, T.B., Yahya, A., & Remigio, P. (2022). Competitive removal of textile dyes from solution by pine bark-compost in batch and fixed bed column experiments. *Environmental Technology & Innovation*, 27, 102421. https://doi.org/10.1016/j.eti.2022.102421
30. Khim, H.C., & Mohd, A.H. (2023). Removal of antibiotics through fixed bed adsorption: Comparison of different breakthrough curve models. *Journal of Water Process Engineering*, 56, 104512. https://doi.org/10.1016/j.jwpe.2023.104512
31. Kishor, R., Purchase, D., Saratale, G.D., Saratale, R.G., Ferreira, L.F.R., Bilal, M., Chandra, R., & Bharagava, R.N. (2021). Ecotoxicological and health concerns of persistent coloring pollutants of textile industry wastewater and treatment approaches for environmental safety. *Journal of Environmental Chemical Engineering*, 9(2): 105012. https://doi.org/10.1016/j.jece.2020.105012
32. Krainer, F.W., & Glieder, A. (2015). An updated view on horseradish peroxidases: Recombinant production and biotechnological applications. *Appl. Microbiol. Biotechnol*, 99, 1611–1625. https://doi.org/10.1007/s00253-014-6346-7.
33. Ladole, M.R., Pokale, P.B., Patil, S.S., Belokar, P.G., & Pandit, A.B. (2020). Laccase immobilized peroxidase mimicking magnetic metal organic frameworks for industrial dye degradation. *Bioresource Technology*, 317, 124035. https://doi.org/10.1016/j.biortech.2020.124035
34. Leon, J.C., Alpeeva, I., Chubar, T., Galaev, I.Y., Csoregi, E., & Sakharov, I.Y. (2002). Purification and substrate specificity of peroxidase from sweet potato tubers. *Plant Science*, 163 (5), 1011-1019. DOI:10.1016/S0168-9452(02)00275-3
35. Madan, S.S., De, B.S., Wasewar, K.L. (2019). Adsorption performance of packed bed column for benzylformic acid removal using CaO_2 nanoparticles. *Chemical Data Collections*, 23, 100267. https://doi.org/10.1016/j.cdc.2019.100267
36. Maghraby, Y.R., El-Shabasy, R.M., Ibrahim, A.H., & Azzazy, H.M.E. (2023). Enzyme Immobilization Technologies and Industrial Applications. *ACS Publications*, 8, 389−396. https://doi.org/10.1021/acsomega.2c07560
37. Maryam, J., Mahmood, R.R., Arash, A., Mehrorang, G., & Hamedreza, J. (2022). Experimental design for the optimization of paraquat removal from aqueous media using a fixed-bed column packed with Pinus Eldarica stalks activated carbon. *Chemosphere*, 291, Part 2, 132670. https://doi.org/10.1016/j.chemosphere.2021.132670
38. Matto, M., Satar, R., & Husain, Q. (2009). Application of calcium alginate–starch entrapped bitter gourd (Momordica charantia) peroxidase for the removal of colored compounds from a textile effluent in batch as well as in continuous reactor. *Applied Biochemistry and Biotechnology*, 158, 512-523. https://doi.org/10.1007/s12010-008-8396-8
39. Miranda, M. E., Moeller, C. G., Villegas, R. O., Buitrón, G., & Garzón, Z. M. (2018). Decolourization of Direct Blue 2 by peroxidases obtained from an industrial soybean waste. *Water,* 44(2), 204-210. https://doi.org/10.4314/wsa.v44i2.06

40. Mohamad, N.R., Marzuki, N.H.C., Buang, N.A., Huyop, F., & Wahab, R.A. (2015). An overview of technologies for immobilization of enzymes and surface analysis techniques for immobilized enzymes. *Biotechnol Equip*, 29 (2): 205-20. https://doi.org/10.1080/13102818.2015.1008192.
41. Munir, A., Nahrir, M.A., Lubis, M.U., Jahangir, A.M.I., Al-Wabel, H.A., Al-Swadi, M., Imran, R., & Abdullah, S.F. (2023). Scavenging microplastics and heavy metals from water using jujube waste-derived biochar in fixed-bed column trials. *Environmental Pollution*, 335, 122319. https://doi.org/10.1016/j.envpol.2023.122319
42. Natália, C., Fontão, F.V., Hackbarth, D.A., Mayer, L.P., Mazur, A.A.U., Souza, V.J.P., Vilar, S.M.A., & Guelli, U.S. (2020). A step forward on mathematical modeling of barium removal from aqueous solutions using seaweeds as natural cation exchangers: Batch and fixed-bed systems. *Chemical Engineering Journal*, 401, 126019. https://doi.org/10.1016/j.cej.2020.126019
43. Olisah, C., Adams, J.B., & Rubidge, G. (2021). The state of persistent organic pollutants in South African estuaries: A review of environmental exposure and sources. *Ecotoxicology and Environmental Safety*, 219, 112316. https://doi.org/10.1016/j.ecoenv.2021.112316
44. Omdehghiasi, H., Yeganeh, B. A., & Korayem, A.H. (2024). Comprehensive study on copper adsorption using an innovative graphene carbonate sand composite adsorbent: Batch, fixed-bed columns, and CFD modeling insights. *Chemical Engineering and Processing - Process Intensification*, 206, 110047. https://doi.org/10.1016/j.cep.2024.110047
45. Pedrajas, J.R., Miranda, V. A., Javanmardy, N., Gustafsson, J.Å., & Spyrou, G. (2020). Mitochondria of Saccharomyces cerevisiae contain one-conserved cysteine type peroxiredoxin with thioredoxin peroxidase activity. *Journal of Biological Chemistry*, 275(21), 16296-16301. DOI: 10.1074/jbc.275.21.16296
46. Qili, H., Qi, H., Danni, Y., & Hengyuan, L. (2021). Prediction of breakthrough curves in a fixed-bed column based on normalized Gudermannian and error functions. *Journal of Molecular Liquids*, 323, 115061. https://doi.org/10.1016/j.molliq.2020.115061
47. Qili, H., Xingyue, Y., Leyi, H., Yixi, L., Liting, H., Qiuming, P., & Xiangjun, P. (2024). A critical review of breakthrough models with analytical solutions in a fixed-bed column. *Journal of Water Process Engineering*, 59, 105065. https://doi.org/10.1016/j.jwpe.2024.105065
48. Rahi, K.A., Al-Madhhachi, A.S.T., & Al-Hussaini, S.N. (2019). Assessment of surface water resources of eastern Iraq. *Hydrology* 6(3): 57. https://doi.org/10.3390/hydrology6030057
49. Rania, Al. T., Sameh, S.A., Fanghua, L., Kamal, M., Okasha, Y.A.G., Mahmoud, T.E., Haixin, J., Yinyi, F., & Jianzhong, S. (2022). A critical review on the treatment of dye-containing wastewater: Ecotoxicological and health concerns of textile dyes and possible remediation approaches for environmental safety. *Ecotoxicology and Environmental Safety*, 231, 113160. https://doi.org/10.1016/j.ecoenv.2021.113160
50. Sevtap, T. (2025). Optimization of coagulation process parameters for reactive red 120 dye using ferric chloride via response surface methodology. *Black Sea Journal of Engineering and Science*. DOI:10.34248/bsengineering.1766799
51. Sikha, S., Shashi, B.S., & Bishnupada, M. (2025). Investigating the efficacy of bimetallic metal-organic frameworks (MOFs) as fluoride adsorbent in fixed-bed adsorption columns: Experimental and modeling insights. *Journal of Water Process Engineering*, 71, 107376. https://doi.org/10.1016/j.jwpe.2025.107376
52. Suppanat, T., Sakonsupa, D., Yothin, C., Manunchaya, J., Nattaporn, T., & Adisak, S. (2025). Valorization of hardboard waste for ciprofloxacin removal: Characterization, adsorption mechanisms, and fixed-bed column analysis. *Chemical Engineering Science*, 312, 121647. https://doi.org/10.1016/j.ces.2025.121647
53. Teba, S.H., & Ayad, A.H.F. (2023). Nanoparticles of (calcium/aluminum/CTAB) layered double hydroxide immobilization onto iron slag for removing of cadmium ions from aqueous environment. *Arabian Journal of Chemistry*, 16(9), 105031. https://doi.org/10.1016/j.arabjc.2023.105031
54. Teba, S.H., Ayad, A.H.F. (2024). Composite sorbent prepared from layered double hydroxide nanoparticles to remediate simulated groundwater polluted with lead and cadmium ions. *Mathematical Modelling of Engineering Problems*, 10(5), 1573-1586. https://doi.org/10.18280/mmep.100509
55. Timothy, G., Myers, A.C., & Abel, V. (2023). On the development of a consistent mathematical model for adsorption in a packed column and why standard models fail. International *Journal of Heat and Mass Transfer*, 202, 123660. https://doi.org/10.1016/j.ijheatmasstransfer.2022.123660
56. Vishwasrao, C., & Ananthanarayan, L. (2018). Kinetics of inactivation of quality-deteriorating enzymes and degradation of selective phytoconstituents in pink guava pulp during thermal processing. *Journal of Food Science and Technology,* 55, 3273-3280. DOI: 10.1007/s13197-018-3262-3
57. Wang, Z., Chen, Z., Chang, J., Shen, J., Kang, J., & Chen, Q. (2015). Fabrication of a low-cost cementitious catalytic membrane for p-chloronitrobenzene degradation using a hybrid ozonation-membrane filtration system. *Chemical Engineering Journal*, 262, 904-912. https://doi.org/10.1016/j.cej.2014.10.033
58. Yang, J.R., Zhang, X.K., Tian, J.H., & Qin, X.Y., (2022). Enhanced Activity of Enzyme Immobilized on Hydrophobic ZIF-8 Modified by Ni^{2+} Ions. *A Journal of the German Chemical Society*, 62. https://doi.org/10.1002/anie.202216699.